Indium distribution and correlations in polymetallic veins from Pingüino deposit, Deseado Massif, Patagonia, Argentina

Sebastián M. Jovic[1,2,*], Diego M. Guido[1,2], Remigio Ruiz[1,2], Gerardo N. Páez[1,2] & Isidoro B. Schalamuk[1,2]

[1]*Instituto de Recursos Minerales (INREMI), Universidad Nacional de La Plata, Argentine*
[2]*Consejo Nacional de Investigaciones Científicas y Técnicas (CONICET), Argentine*
**Corresponding author (e-mail: sjovic@inremi.unlp.edu.ar)*

ABSTRACT: The Pingüino deposit is characterized by the presence of indium-rich polymetallic vein mineralization representing an atypical epithermal occurrence for the low sulphidation epithermal mineralization from the Deseado Massif, Patagonia, Argentina. Polymetallic veins display high In, Zn, Pb, Ag, Cd, Au, As, Cu, Sn, W and Bi values represented by complex sulphide mineralogy. Mineralization developed in two main stages: a Cu-Au-In-As-Sn-W-Bi stage, and a Zn-Pb-Ag-In-Cd-Sb stage. Correlation coefficients are used to estimate the degree of inter-relation between metals concentrations in each stage and specifically to determinate the behaviour of indium. Indium concentrations show a wide range (3.4–1184 ppm In) and, based on the correlation coefficients of ore geochemistry, in the first stage indium is associated mainly with Sn, present in ferrokesterite and cassiterite, while the highest indium values are related to the late mineralization stage, closely associated with Zn and Cd and present in the Fe-rich sphalerite, the most important In-bearing mineral in the deposit.

KEYWORDS: *Ore geochemistry, indium, metallogenesis, Deseado Massif, Argentina*

The Deseado Massif is located in the Santa Cruz province in southern Argentinean Patagonia (Fig. 1a) and is characterized by the presence of low sulphidation epithermal deposits that are spatially, temporally and genetically related to a complex and long-lived (more than 30 Ma) Jurassic magmatic event associated to tectonic extension (Guido & Schalamuk 2003).

The Deseado Massif is an important Au–Ag producer with four operational mines (Cerro Vanguardia, Mina Martha, San José and Manantial Espejo), and is also the subject of intense prospecting activities with more than 50 mining projects. Mineralization consists mainly of quartz veins and veinlets, vein stockworks and hydrothermal breccias hosted mainly in Jurassic volcanic rocks. The dominant mineralization trend is NW–WNW, with minor NE and E–W. Quartz textures are commonly massive, brecciated, crustiform and colloform banding with comb, cockade and lattice bladed texture (Dong *et al.* 1995). Metalliferous minerals in the quartz veins are commonly less than 1% in volume. They are mainly pyrite, native gold, electrum, argentite, native silver, Ag-sulphosalts, hematite, sphalerite, galena, and chalcopyrite. The geochemical signature is characterized by anomalous precious metals (Au–Ag) and locally anomalous contents of As, Sb, Hg, Mo, Pb, Zn, Mn, and minor Cu (Guido & Schalamuk 2003).

In recent years, some atypical (different to low sulphidation type) epithermal occurrences have been discovered in the Deseado Massif. Mina Martha is an example, being a Ag-rich deposit with a Ag:Au ratio of 1000:1 and high contents of base metals. These characteristics led Gonzalez Guillot *et al.* (2004) to include it into the intermediate sulphidation type of Hedenquist *et al.* (2000).

Pingüino is another atypical epithermal deposit in the Deseado Massif (Guido *et al.* 2005), located in the central portion of region, 40 km to the NW from the Cerro Vanguardia mine (Fig. 1a). This deposit is characterized by the presence of two different vein types, early polymetallic sulphide-rich veins and late quartz-rich Ag–Au veins. The polymetallic veins show important anomalies of In as well as Zn, Pb, Ag, Au, Cu, Sn, W and Bi (Guido *et al.* 2005).

The deposit contains 35.4 million tonnes at 4.0 oz/t silver equivalent in inferred category and 7.32 million tonnes at 5.5 oz/t silver equivalent in indicated category (silver equivalent = Ag+Au+Pb+Zn+In; Argentex 2009).

The occurrence of indium minerals is very rare, and generally In substitutes in base metal sulphide minerals for elements with similar ionic radii. The most common In-bearing minerals are: sphalerite where In is substituting for Zn and Fe, stannite, kesterite, ferrokesterite and cassiterite where In replaces Sn and Fe (Schwarz-Schampera & Herzig, 2002).

The aim of this contribution is to study the metals' distribution and correlation, and specifically to analyse the behaviour of In in the polymetallic mineralization of the Pingüino deposit sulphide veins.

GEOLOGICAL SETTING OF THE PINGÜINO DEPOSIT

The oldest rocks in the study area are Middle to Upper Triassic continental sedimentary rocks of El Tranquilo Group (Jalfin & Herbst 1995; Fig. 1b); these are fine to coarse sandstones with

Geochemistry: Exploration, Environment, Analysis, Vol. **11** 2011, pp. 107–115
DOI 10.1144/1467-7873/09-IAGS-013

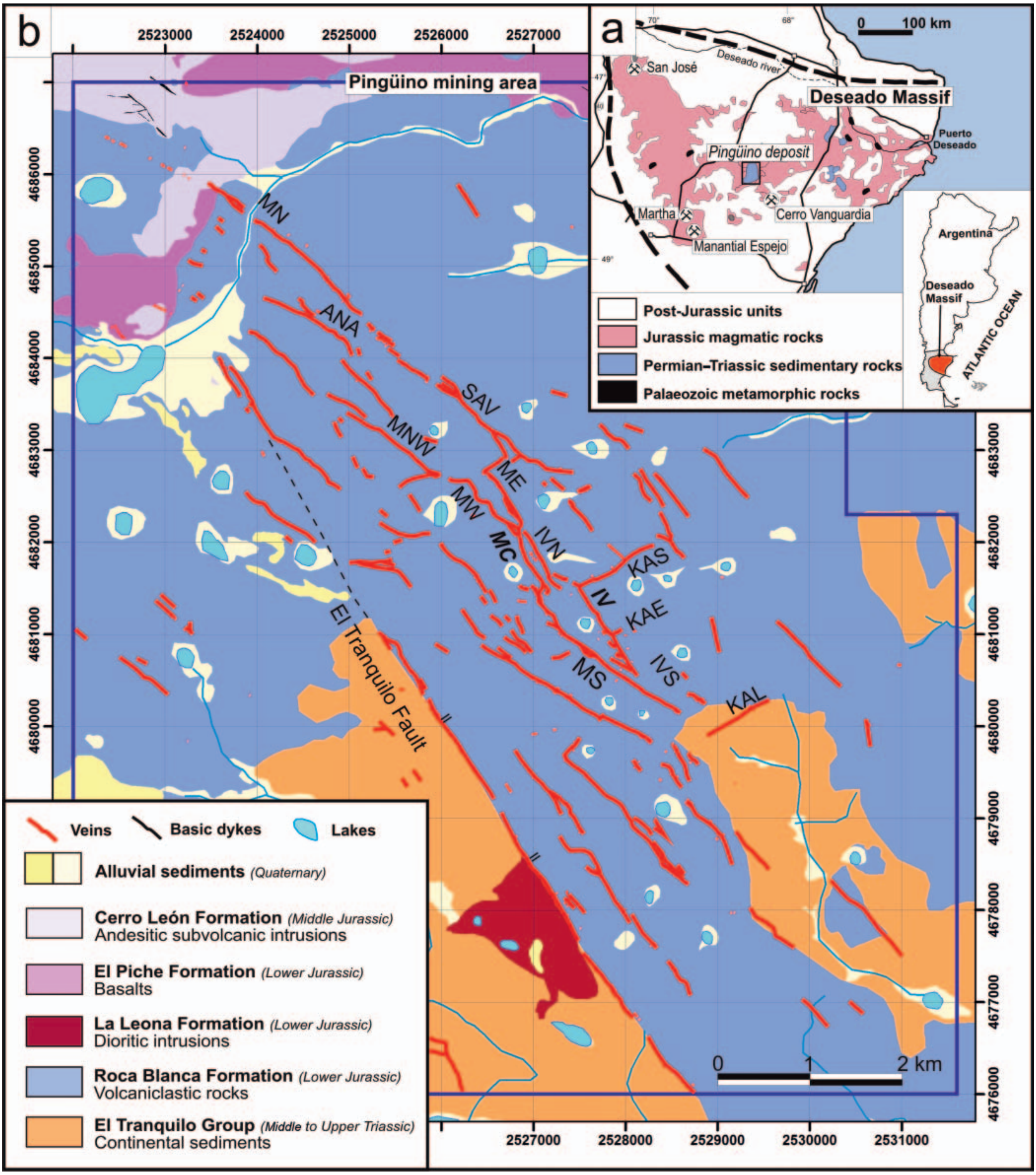

Fig. 1. (**a**) Simplified geological map of the Deseado Massif showing the location of the Pingüino deposit. (**b**) Simplified geological and vein map of the Pingüino deposit. Main veins: MN, Marta Norte; ANA, Ana; SAV, Savary; MNW, Marta Noroeste; ME, Marta Este; MW, Marta Oeste; MC, Marta Centro; IVN, Ivonne Norte; IV, Ivonne; KAS, Kasia; MS, Marta Sur; IVS, Ivonne Sur; KAL, Kalia.

volcanic components and rhythmic alternation of siltstones, mudstones, black shales and coal levels. Dioritic intrusive bodies, with associated mafic sills and dikes, assigned to the Lower Jurassic La Leona Formation (Jovic 2009), intrude the Triassic rocks. The Lower Jurassic Roca Blanca Formation (Herbst 1965) is composed of epiclastic and pyroclastic fine sandstones to conglomerate and tuffitic rocks, volcanic sandstones and some tuffaceous levels and minor ignimbrite deposits. Basaltic lava flows from El Piche Formation (Jovic 2009) crop out in the northern sector of the area, intercalated within the volcaniclastic rocks of the Roca Blanca Formation. In the northwestern sector, the sequence is intruded by andesitic subvolcanic bodies, assigned to the Middle Jurassic Cerro León Formation (Panza 1995).

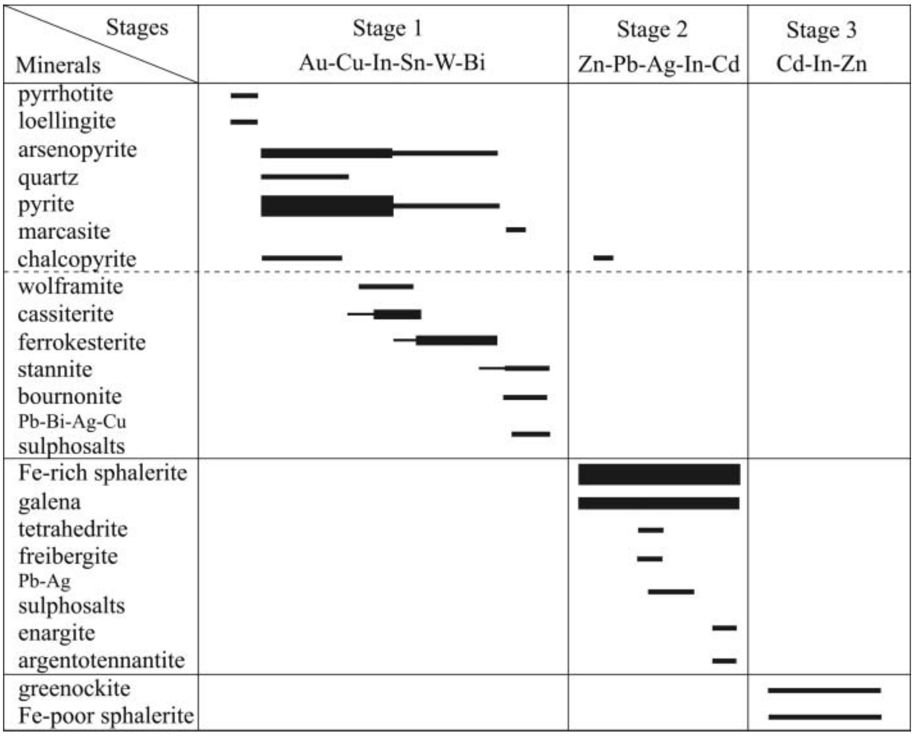

Fig. 2. Paragenetic diagram of the sulphide veins from Pingüino deposit.

Different deformation scales and styles can be recognized in the area, including a regional structural dome (15–20 km in diameter) with radial faulting, kilometric transverse fault and fracture systems and localized minor scale folding structures (<1 km). Peñalva *et al.* (2008) proposed that a deep intrusion (3 km deep) is responsible for the regional doming and the radial fracture system. The El Tranquilo Fault (325°) is the principal brittle structure, and is associated to the east with secondary extensional faults (Jovic *et al.* 2005). Folded structures (domes <1 km) represent local deformation associated to, generally not-outcropping, andesitic subvolcanic bodies and dioritic intrusions that have been confirmed by regional magnetometric surveys (Peñalva *et al.* 2008) and exploration drill holes (Cortiñas *et al.* 2005; Argentex 2009).

The Pingüino deposit is 74 km long and occupies a fault system with NW and ENE strike, hosted in Triassic continental sedimentary rocks and Lower Jurassic epiclastic and volcanoclastic rocks. These veins are arranged in an extensional sinistral strike slip duplex system, where, three main orientations can be recognized: the El Tranquilo vein system (330–325°), the Marta vein system (300–310°), and the Kasia vein system (260–250°). El Tranquilo and Marta vein systems comprise the main veins, where the most important ore shoots are developed: Marta Norte, Marta Noroeste, Savary, Marta Este, Marta Oeste, Marta Centro, Ivonne Norte, Marta Sur, Ivonne, and Ivonne Sur. The K system also develops ore shoots when they are close to the Marta veins system; Kasia, Kae and Kalia veins are the most important within this system (Fig. 1b).

The deposit is characterized by the presence of two vein types, early polymetallic sulphide-rich veins and late quartz-rich veins. The polymetallic mineralization is characterized by massive sulphide veins and breccias up to 13 m thick with a Sn, W, Cu, Au, As, Bi, Zn, Pb, Ag, In, Cd and Sb geochemical signature. Quartz mineralization is represented by breccias and veins with a maximum thickness of 20 m composed of quartz, carbonates, clays and some sulphides with colloform and crustiform banding, comb, cockade and minor lattice bladed textures. These veins have high Ag (from 0.4–1561 ppm; n=77), Au (from 0.02–8.67 ppm; n=77) values and Ag:Au ratios (400:1, n=77), and are devoid of the polymetallic metal association present in the sulphide veins. Late quartz-rich Ag–Au veins crosscut the early polymetallic sulphide-rich veins providing evidence of the overlapping of two different mineralization styles in the same fault system. Quartz-rich veins present similar characteristics with the typical low sulphidation type mineralization from the Deseado Massif (Jovic 2009).

The main sulphide veins (Ivonne, Ivonne Norte, Ivonne Sur, Marta Centro, Kasia) are located in the centre of the deposit (Fig. 1b) above a (not-outcropping) dioritic intrusion that was confirmed by magnetometric surveys (Peñalva *et al.* 2008) and exploration drill holes (Argentex 2009), indicating a spatial relation between the sulphide veins and the dioritic intrusions. The age of dioritic intrusions was dated by Sm/Nd in 194 Ma (Jovic 2009) while $^{207}Pb/^{204}Pb$ vs. $^{206}Pb/^{204}Pb$ data of sulphide ore minerals show a good correlation defined by a line that intercepts the Pb isotopic evolution curve at 193 Ma, indicating a Lower Jurassic age for the mineralization (Jovic 2009). These ages show a contemporaneous magmatic activity with the hydrothermal system that formed the polymetallic mineralization, indicating a temporally relation between them.

POLYMETALLIC MINERALIZATION

The polymetallic veins are poorly exposed at surface and are characterized by the presence of gossans with remnants of breccias with quartz matrix and oxidized sulphide clasts. These gossans are represented by a high concentration of limonite, red clays and penetrative pyritization. The mineralogy is characterized by goethite, reddish kaolinite, dickite, nacrite, Pb supergenic minerals such as plumbojarosite ($PbFe_6(SO_4)O_{12}$) and plumbonacrite ($Pb_{10}(CO_3)_6O(OH)_6$); soil and trench geochemistry shows anomalies of Fe, Pb, Cd, In and Bi, Cu, Au, As, Sb. These gossans represents the oxidation of sulphide veins and build an oxidation zone that ranges between −30 to −60 m in depth.

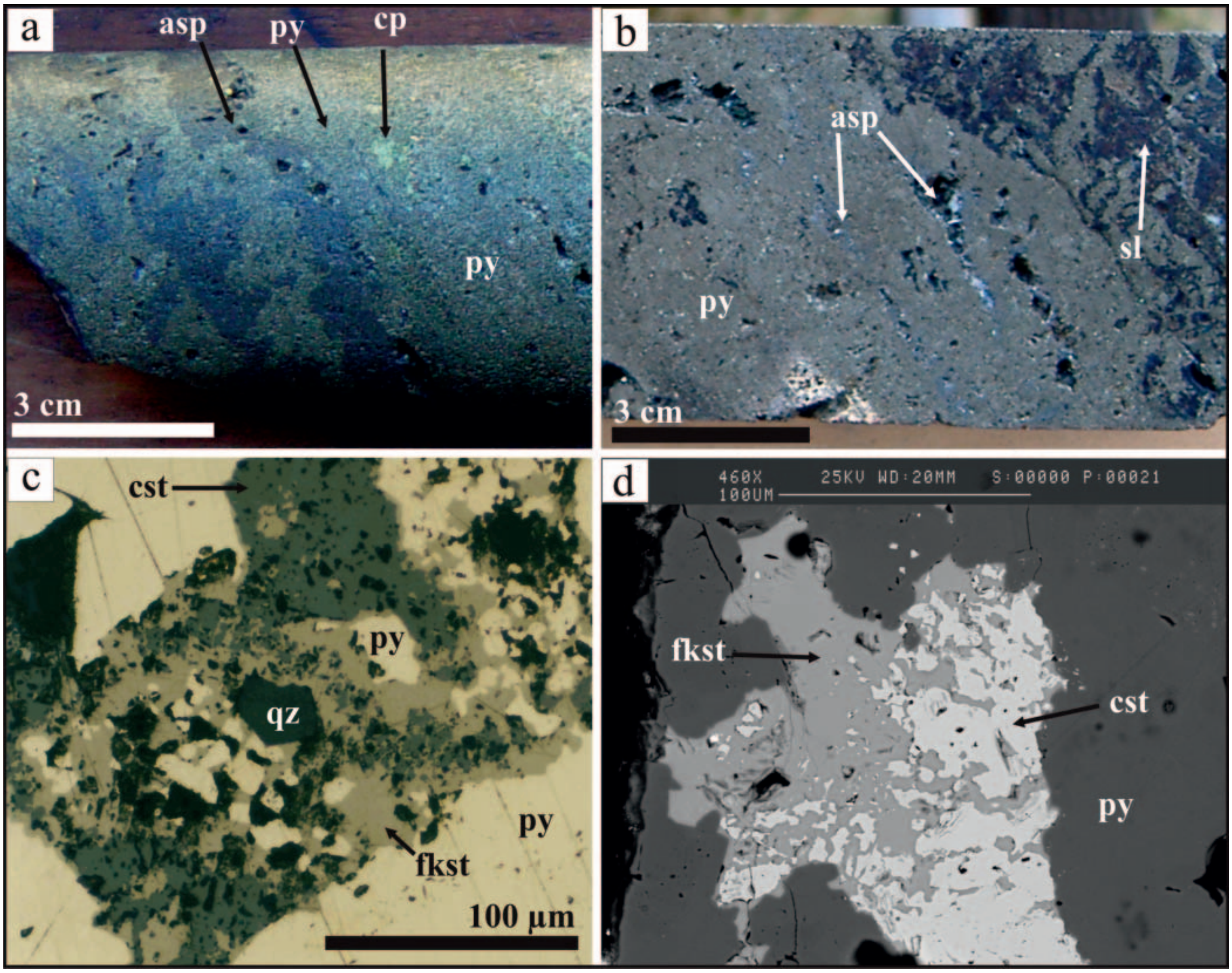

Fig. 3. Main textural relationships of the first mineralization stage in the Ivonne vein. (**a**) Massive to banded pyrite (py), arsenopyrite (asp) and chalcopyrite (cpy) vein. (**b**) Pyrite (py) and arsenopyrite (asp) crosscut by Fe-rich sphalerite (Fe-rich sl). (**c**) Microphotograph from a polished section showing pyrite (py) and quartz (qz) crystals brecciated by cassiterite (cst) and ferrokesterite (fkst). (**d**) Backscattered images of ferrokesterite (fkst) replacing cassiterite (cst).

Hypogene polymetallic mineralization is characterized by the presence of massive and banded sulphide veins and breccias up to 13 m thick. This mineralization is developed in three stages (Fig. 2).

The first stage (Fig. 3) is composed mainly by idiomorphic pyrite crystals, zoned arsenopyrite crystals up to 1 cm in size and hipidiomorphic chalcopyrite crystals between 10 µm and 2 mm. Minor small (<50 µm) crystals of löllingite *($FeAs_2$)* and pyrrhotite are present and were replaced by pyrite and arsenopyrite. Cassiterite is present as alotriomorphic and idiomorphic crystals up 200 µm that are filling fractures. Radial aggregates of idiomorphic hübnerite *($MnWO_4$)* crystals (<1 mm) are associated with the cassiterite. Ferrokesterite *($Cu_2(Fe,Zn)SnS_4$)* replaces cassiterite, and is in turn replaced by stannite *(Cu_2FeSnS_4)*. Very fine grain (<50 µm) acicular and prismatic Ag–Bi, Ag–Pb–Bi, Pb–Bi sulphosalts such as aramayoite *($Ag(Sb,Bi)S_2$)*, owyheeite *($Pb_7Ag_2(Sb,Bi)_8S_{20}$)*, ourayite *($Pb_4Ag_3Bi_5S_{13}$)*, giesenite *($Cu_2Ag_{26}(Sb,Bi)_{20}S_{57}$)* and izoklakeite *($Pb_{27}(Cu,Fe)_2(Sb,Bi)_{19}S_{57}$)* are present late in this stage. Minor amounts of marcasite, bournonite *($PbCuSbS_3$)* and quartz are also recognized. This stage is best represented in the Ivonne vein (Jovic *et al.* 2005; Crespi 2006).

In the second stage (Fig. 4), minerals from the early stage were brecciated and replaced mainly by banded sphalerite and galena. The most abundant mineral in this stage is the sphalerite with alotriomorphic to idiomorphic crystals up to 2 cm. Galena is very abundant and is present in irregular masses or idiomorphic crystals up to few centimetres, and it is intergrown with the sphalerite. Tetrahedrite and freibergite grains between 100–500 µm, argentotennantite (< 20 µm) and Pb–Ag sulphosalts (< 20 µm) are present in this stage. Minor late enargite grains (<50 µm) are present in the galena cleavage planes or as irregular masses related with freibergite. This stage is best developed in the Marta Centro vein (Jovic *et al.* 2005; Crespi *et al.* 2006).

A third mineralization stage was recognized only by microscope (Fig. 5) and is characterized by a sequences of botryoidal Fe-poor sphalerite followed by small (<25 µm) idiomorphic crystals of greenockite. This stage is represented in Ivonne and Marta Centro veins (Jovic *et al.* 2005; Crespi 2006).

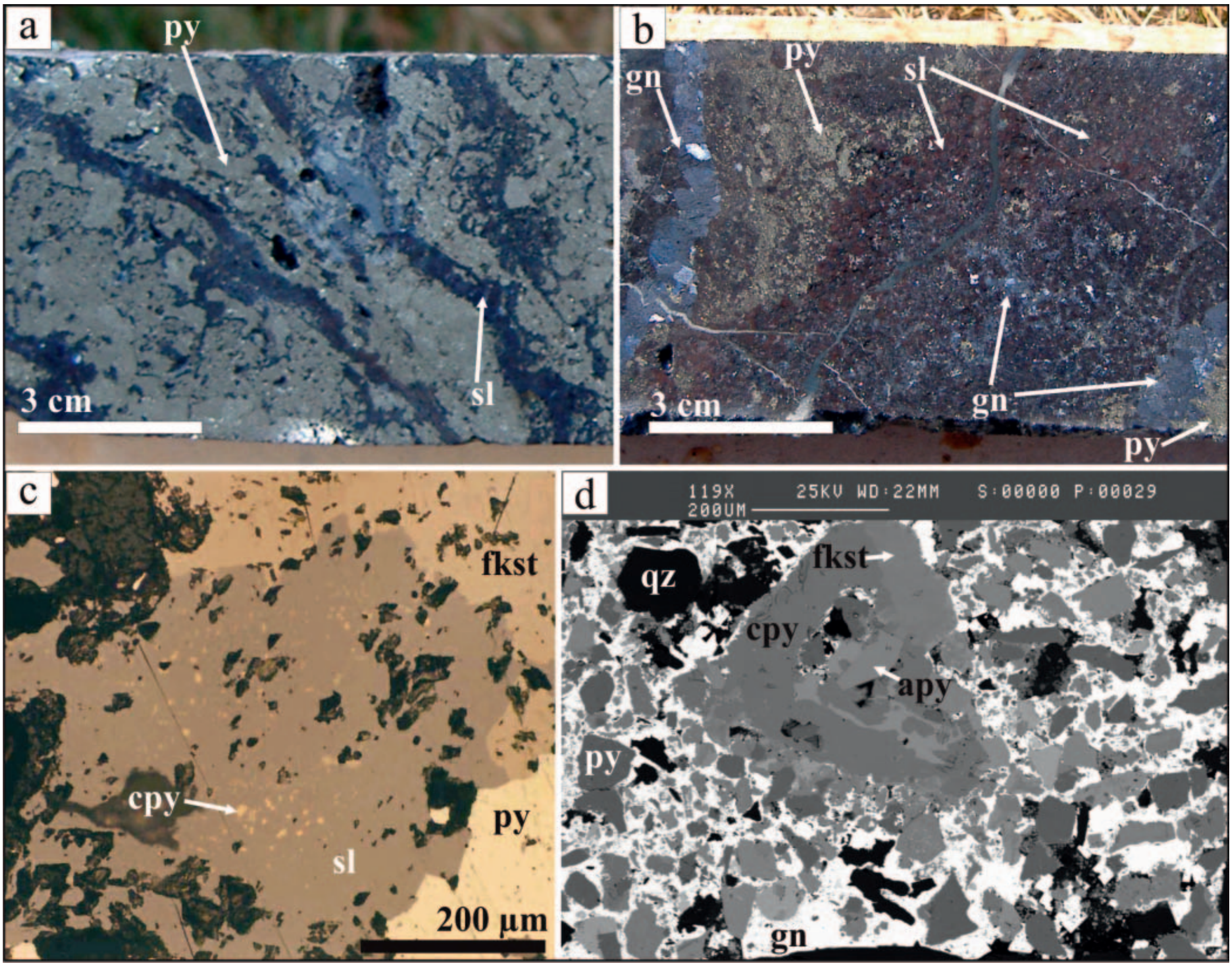

Fig. 4. Main textural relationships of the second mineralization stage in the Marta Centro vein. (**a**) Fe-rich sphalerite (Fe-rich sl) veinlets crosscutting pyrite (py) vein. (**b**) Banded Fe-rich sphalerite (Fe-rich sl) and galena (gn) breccia with pyrite (py) clasts. (**c**) Microphotograph from a polished section showing Fe-rich sphalerite (Fe-rich sl) crystal with chalcopyrite inclusions, and pyrite (py) and ferrokesterite (fkst) crystals. (**d**) Backscattered images of galena (gn) breccia with pyrite (py), arsenopyrite (apy), chalcopyrite (cp), ferrokësterite (fkst), and quartz (qz) clasts.

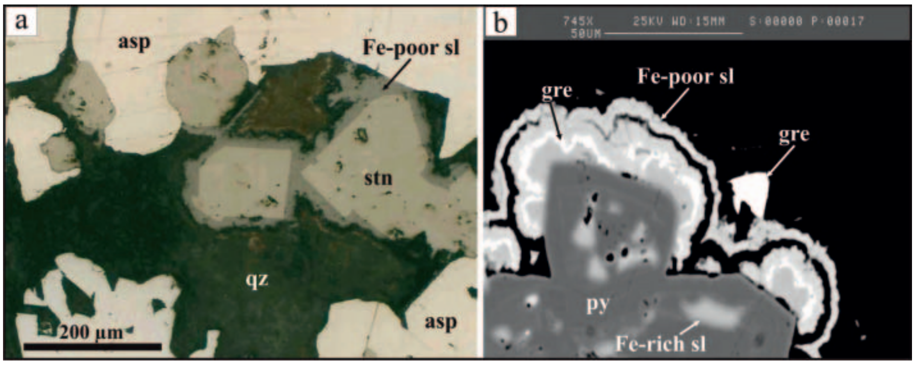

Fig. 5. Main textural relationships of the third mineralization stage in the Ivonne and Marta Centro veins. (**a**) Microphotograph from a polished section showing stannite (stn) and idiomorphic greenockite (gre) crystals surrounded by botryoidal banded Fe-poor sphalerite (Fe-poor sl). (**b**) Botryoidal banded Fe-poor sphalerite (Fe-poor sl) and greenockite (gre) surrounding a pyrite (py) crystal with Fe-rich sphalerite (Fe-rich sl) and an idiomorphic greenockite (gre) crystal over the botryoidal banded.

ORE GEOCHEMISTRY

The hypogene high-grade ore shoots zones, developed between −30 m to −120 m, from the Ivonne and Marta Centro veins were studied. These veins are 1000 m and 700 m in length and average 3 m and 7 m in thickness, respectively, and were drilled up to −400 m.

Representative samples from the different mineralizing stages were analysed at Acme Analytical Laboratories (Chile-Canada) by instrumental neutron activation analyses (INAA), inductively coupled plasma-atomic emission spectroscopy (ICP-AES), and inductively coupled plasma-mass spectrometry (ICP-MS); for detailed analytical methodology see http://acmelab.com/.

The studied samples are from the Ivonne vein (n=45) representing the first polymetallic stage and from the Marta Centro vein (n=100) representing the second polymetallic stage. The average, maximum and minimum values of major

Table 1. *Summary of geochemistry analyses for polymetallic sulfide veins of the Pingüino deposit. I: Ivonne. M.C.: Marta Centro. Ps_1: First polymetallic mineralization stage. Ps_2: Second polymetallic mineralization stage*

Stage	Values	In ppm	Au ppm	Ag ppm	Cu wt.%	Pb wt.%	Zn wt.%	Sn ppm	Bi ppm	Cd ppm	As wt.%	Sb ppm	W ppm
I. vein	Average	49.6	2.77	45.5	0.41	0.13	1.27	1267	93.9	61.7	1.00	66.5	55.2
Dominantly Ps_1	Maximum	159.4	8.07	237.0	2.47	0.30	6.10	5961	390.8	338.2	4.41	509.1	740.0
n = 45	Minimum	3.4	0.01	2.6	0.01	0.01	0.02	7	0.8	3.6	0.02	1.4	0.2
M. C. vein	Average	161.8	0.74	156.3	0.14	3.65	10.81	153	5.3	848.5	0.40	87.0	2.4
Dominantly Ps_2	Maximum	1184	1.34	684.0	5.99	19.30	32.95	564	30.1	14900	1.28	634.8	25.2
n = 100	Minimum	5.25	0.10	14.5	0.01	0.16	0.08	23	0.1	6.0	0.07	5.0	0.1

Table 2. *Correlation matrix for metals of the first polymetallic mineralization stage in the Ivonne vein*

	In	Au	Ag	Cu	Pb	Zn	Sn	Bi	Cd	As	Sb
Au	0.67										
Ag	0.70	0.69									
Cu	0.67	0.66	0.84								
Pb	0.67	0.59	0.77	0.64							
Zn	0.40	−0.08	0.35	0.18	0.48						
Sn	0.77	0.82	0.64	0.54	0.63	−0.03					
Bi	0.67	0.69	0.83	0.63	0.50	0.22	0.52				
Cd	0.60	0.33	0.57	0.38	0.83	0.71	0.49	0.27			
As	0.31	0.61	0.50	0.24	0.34	0.02	0.34	0.59	0.23		
Sb	0.77	0.80	0.81	0.72	0.62	0.07	0.76	0.74	0.38	0.48	
W	0.50	0.71	0.41	0.47	0.52	−0.17	0.82	0.34	0.26	0.08	0.67

(Zn, Pb, Cu, As), and trace element contents (Au, Ag, Sb, Bi, Sn, In, Cd, W) are listed in Table 1.

The ore geochemistry indicates the presence of high values of Cu, Au, As, Sn, W, Bi, Zn, Pb, Ag, In, Cd, and Sb in the polymetallic veins. Major and minor element associations reflect the two different mineralogical assemblages: an assemblage related with the Stage 1 is characterized by anomalous values of Au, Cu, Sn, Bi, As and W, whereas the highest values of Zn, Pb, In, Ag, Cd and Sb are present in Stage 2 (Table 1).

In order to estimate the degree of correlation between metals concentration on each mineralizing stage, the correlation coefficient 'r' was calculated (Davis 1986). They are shown in Table 2 for the first stage and Table 3 for the second stage.

In the first stage, many of the elements show moderate to high degrees of correlation with each other (Table 2). Indium's highest concentrations (up to 160 ppm) strongly correlate with Sn (Table 2, Fig. 6a) and Sb, but also correlate with Au, Ag, Cu, Pb, Bi and Cd and moderate correlation is evident with W, Zn and As.

Gold presents the highest values (up to 8 ppm) and correlates with Sn, W (Table 2, Fig. 6b, 6c) and Sb. Tin and W show high values in this stage (up to 5961 ppm Sn and 740 ppm W) and a strong correlation (Table 2, Fig. 6d), while Ag is clearly associated with Bi, Sb, Cu (Table 2, Fig. 6e, 6f) and Pb.

Indium's highest values are present in the second stage (up to 1184 ppm) and show a strong correlation with Zn (Table 3, Fig. 7a) and Cd (Table 3, Fig. 7b) but also with Sn (Table 3, Fig. 7c). Zinc and Cd present a high correlation (Table 3, Fig. 7d) showing an important relation amongst In, Zn and Cd. Silver, Pb and Sb have the highest concentrations in this stage and show a strong correlation amongst them (Table 3, Fig. 7e, 7f).

DISCUSSION

Indium-bearing polymetallic vein-type deposits are characterized by multiple vein mineralization and characteristic mineral and metal zonation, presenting ores which are complex in mineralogical composition and show an intense telescoping. The typical indium mineralogy is dominated by solid solutions involving sphalerite, stannite, ferrokesterite, cassiterite, chalcopyrite, tetrahedrite, and minor roquesite, roquesite-sphalerite solid solution and sakuraiite (Schwarz-Schampera & Herzig 2002).

Ohta (1995) defined a common sequence of mineralization stages for many In polymetallic deposits in Japan and Bolivia, despite their different geochemical signatures: an early Sn–W stage with cassiterite, wolframite, arsenopyrite and minor pyrrhotite; a second Sn–In stage characterized by stannite, chalcopyrite and minor marcasite and sphalerite; and a final Ag–Pb–Sn stage with Ag sulphosalts and minor Ag–Sn and Pb–Sn minerals.

In the Freiberg district, Germany, the polymetallic sulphide vein-type mineralization is characterized by anomalous concentrations of As(-Au)-Zn-Cu(-In-Cd)-Sn-Pb-Ag-Bi-Sb with arsenopyrite, pyrite/marcasite (minor native Au), pyrrhotite, mostly Fe-rich sphalerite, stannite, chalcopyrite, cassiterite, tetrahedrite, bornite, and galena (Seifert & Sandmann 2006). A sequence of three mineral pulses was recognized: an early Fe–As pulse, a Zn–Sn–Cu stage with high concentrations of In (indium stage) and a late Pb–Ag pulse. Sphalerite from the Zn–Sn–Cu stage is the most important indium-host mineral but In is also related to microscopic Zn–Cu–Sn–In–S grains.

Polymetallic mineralization from the Pingüino deposit shows anomalous values of Au, Cu, In, Sn, W, and Bi in the first stage indicating the precipitation of high temperature mineralization that are represented by a complex sulphide-rich mineralogy. In a general way, the correlations amongst Ag–Pb–Bi–Sb suggest the presence of different Ag–Pb–Bi sulphosalts; correlation amongst Ag–Cu–Sb is represented by freibergite, argentotenantite, and tetrahedrite, while Sn–W is related to wolframite and cassiterite, and the In–Sn–Sb correlation with ferrokesterite, stannite and cassiterite.

Indium anomalies in the first mineralization stage (up to 159 ppm) are related to Sn minerals, mainly ferrokesterite and cassiterite, probably with substitution of Cu and Sn for In in the ferrokesterite, and substitution of Sn for In in the cassiterite. Microprobe analyses in this minerals (Crespi 2006; Jovic 2009) indicated that the highest In content occurs in the ferrokesterite with values that range between 0.04 and 3.02 wt.% (0.52 wt.% in average, n=52), followed by cassiterite with values that vary between 0.14 and 0.36 wt.% (0.22 wt.% in average, n=16). Chalcopyrite does not concentrate significant amounts of In (up to 0.10 wt.%, n=11).

Many of the elements from the first stage show moderate to high degrees of correlation with each other. Indium displays strong correlation not only with Sn and Sb, but also with Au, Ag, Cu, Pb, Bi, and Cd, and moderate correlation with W, Zn, and As. These correlations indicate that various minerals containing these elements, including In, are all closely associated

Table 3. *Correlation matrix for metals of the second polymetallic mineralization stage in the Marta Centro vein*

	In	Au	Ag	Cu	Pb	Zn	Sn	Bi	Cd	As	Sb
Au	0.06										
Ag	0.19	0.21									
Cu	−0.07	0.00	−0.02								
Pb	0.17	−0.03	0.74	−0.09							
Zn	0.77	0.21	0.27	−0.16	0.39						
Sn	0.71	−0.03	0.46	−0.03	0.35	0.58					
Bi	0.56	0.06	0.09	0.39	−0.01	0.35	0.36				
Cd	0.80	0.26	0.23	−0.09	0.22	0.82	0.67	0.44			
As	0.05	−0.08	0.22	−0.09	0.37	0.17	0.10	0.01	0.11		
Sb	0.07	−0.02	0.81	−0.10	0.89	0.27	0.33	−0.09	0.16	0.37	
W	0.28	−0.03	0.07	0.38	−0.01	0.10	0.25	0.31	0.12	0.03	−0.01

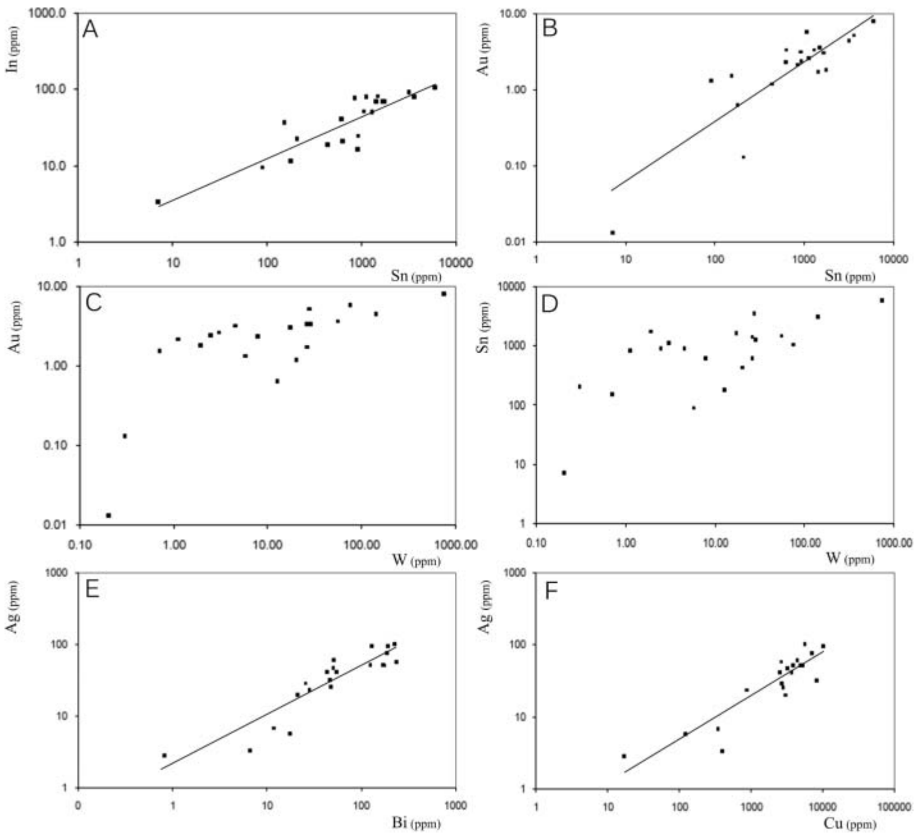

Fig. 6. Selected binary variation diagrams for polymetallic sulphide ores from the first mineralization stage (n=45) in the Ivonne vein.

and intergrown reflecting the complex sulphide mineralogy paragenesis present in this stage.

The highest In grades in the deposit (up to 1184 ppm) are related to the second mineralization stage characterized by anomalous values of Zn–Pb–Ag–In–Cd. Indium and Cd are present in the sphalerite (Crespi 2006), showing a high correlation amongst In–Zn–Cd. Microprobe analyses of sphalerites (Crespi 2006; Jovic 2009) show important concentration of In with values that vary between 0.01 and 2.56 wt.%, (0.47 wt.% in average; n=10) and high contents of Fe (8.29 wt.% in average; n=10), Sn (0.52 wt.% in average; n =10), and Cd (0.50 wt.% in average; n=10). Sphalerite is one of the most abundant minerals in the deposit and is the main In-bearing mineral.

Indium also shows a high correlation with Sn in this stage, but in this case it is not related with the late ferrokesterite that does not concentrate significant amounts of In with values that vary between 0.04 and 0.16 wt.% (0.09 wt.% in average, n=4). This correlation could be explained by the close association between Sn-bearing minerals and sphalerite. The presence of Ag–Pb sulphosalts is responsible for the high correlation between these elements.

Microprobe analyses of minerals from the third mineralization stage (Crespi 2006; Jovic 2009) show that sphalerite presents very low Fe values (0.49 wt.% in average, n=12) and only traces of In (0.06 wt.% in average, n=12) in comparison with the sphalerites from the second stage, while important In contents are concentrated in the greenockite with values that range between 1.92 and 3.63 wt.% (3.07 wt.% in average, n=5). These values represent the highest In contents in the minerals of the polymetalic mineralization. In spite of these high values, this stage of mineralization is volumetrically irrelevant, and hence its contribution to the In grade of the ores is not significant. These high In values could have been produced by removilization of the existing ores (Jovic 2009).

Geochemical signature, sequence of mineralization, mineralogy, In contents, and In-host minerals of the polymetallic mineralization from Pingüino deposit are similar and could be comparable with indium-polymetallic deposits such as Toyoha in Japan, Bolivar in Bolivia (Ohta 1995) and the Freiberg

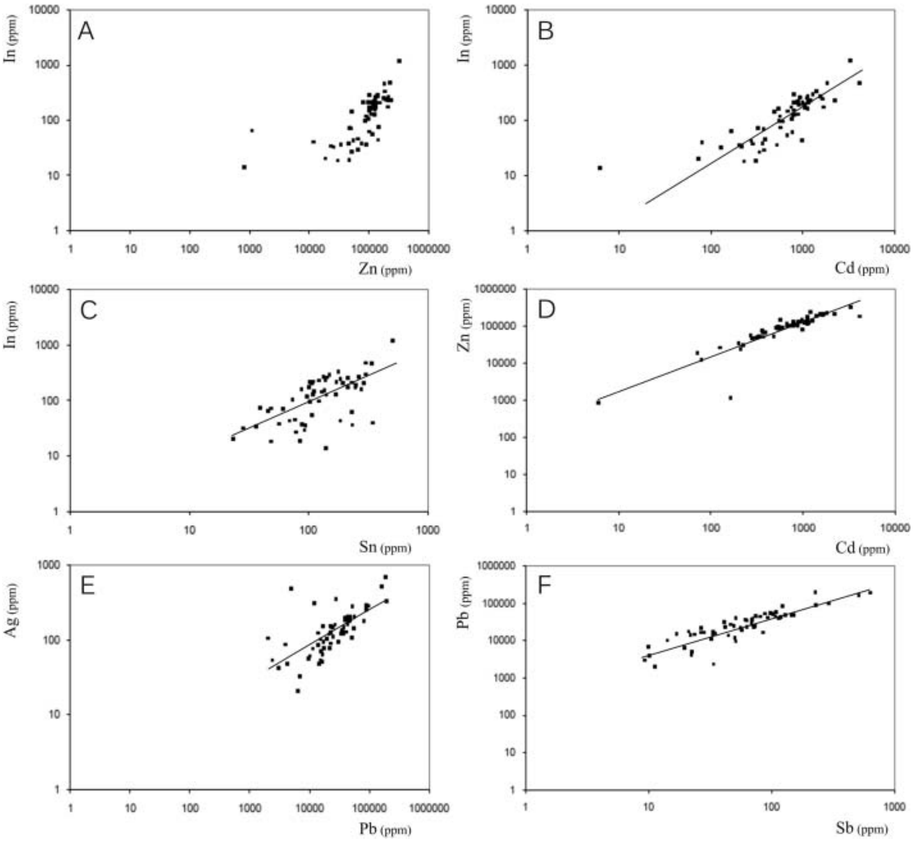

Fig. 7. Selected binary variation diagrams for polymetallic sulphide ores from the second mineralization stage (n=100) in the Marta Centro vein.

district in Germany (Seifert & Sandmann 2006), facilitating its classification as an indium-bearing polymetallic deposit according to Schwarz-Schampera & Herzig (2002).

CONCLUSIONS

The distribution and correlations of the metals in the veins reflects the mineralogical differences of the two main mineralizing stages defined for polymetallic veins at the Pingüino deposit: an early polymetallic stage characterized by the presence of Sn sulphides, Ag–Pb–Bi sulphosalts and Ag–Cu sulphosalts with the highest concentration of Cu, Au, As, Sn, W and Bi; and a second mineralization stage that shows the highest values of Zn, Pb, Ag, In, Cd and Sb with Fe-rich sphalerite, galena and Ag–Pb sulphosalts.

Indium is present in the two main stages, but is concentrated in the second stage related mainly with Zn in the Fe-rich sphalerite, being the most abundant and important In-bearing mineral in the deposit.

For the first mineralization stage, In is associated with Sn, and is present in ferrokesterite and cassiterite but Sn-bearing minerals are not as abundant as sphalerite. A third mineralization stage, produced by remobilization of the existing ores, concentrated high contents of In in the greenockite, but is volumetrically irrelevant and not significant for the In grade of the ores.

The presence of high values of In and other atypical elements for epithermal deposits, such as Sn, W, Bi, Cd and Sb in the polymetallic veins from the Pingüino deposit, represents a new geochemical signature for the epithermal deposits from the Deseado Massif and hence it is classified as an In-bearing polymetallic deposit, similar to the In-bearing polymetallic veins from Japan, Bolivia and Germany.

This contribution forms part of the senior author's PhD thesis at the Universidad Nacional de La Plata, Argentina. The geochemical information that made this work possible was generously provided by Argentex Mining Corporation, we thank the company and its president (Ken Hicks) for the constant support. Thomas Seifert and Dave Sinclair are thanked for very constructive reviews.

REFERENCES

ARGENTEX MINING CORPORATION. 2009. *National Instrument 43-101-compliant mineral resource estimate.* http://www.argentexmining.com

CRESPI, A. 2006. *Estudi mineralògic dels dipòsits del massìs de el Deseado (Argentina).* Unpublished PhD Thesis, Universitat de Barcelona.

CRESPI, A., JOVIC, S.M., GUIDO, D.M., PROENZA, J., MELGAREJO, J.C. & SCHALAMMUK, I.B. 2006. El prospecto Cerro León, Macizo del Deseado, Patagonia, Argentina: Un depósito de Ag-Sn. *Macla*, **6**, 143–145.

CORTIÑAS, J., HOMOVC, J., LUCERO, M., GOBBO, E., LAFFITTE, G. & VIERA, A. 2005. Las cuencas de la región del Deseado, provincia de Santa Cruz. En "Frontera exploratotia de la argentina". *In:* CHEBLI, A.G., CORTIÑAS, J.S., SPALLETTI, L.A., LEGARRETA, L. & VALLEJO, E.L. (eds) *Buenos Aires.* Instituto Argentino del Petróleo y del Gas, 2005, **352**, 289–305.

DAVIS, J. 1986. *Statistics and data analysis in geology.* Second edition. John Wiley & Sons, Inc. New York.

DONG, G., MORRISON, G. & JAREITH, S. 1995. Quartz textures in epithermal veins in Queensland: Classification, origin and implication. *Economic Geology, Scientific Communications*, **90**, 1841–1856.

GONZALEZ, GUILLOT M., DE BARRIO, R. & GANEM, F. 2004. *Mina Martha, un yacimiento epitermal en el Macizo del Deseado, provincia de Santa Cruz.* VII Congreso de Mineralogía y Metalogenia, Córdoba, 199–204.

GUIDO, D.M. & SCHALAMUK, I.B. 2003. Genesis and exploration potential of epithermal deposits from the Deseado Massif, Argentinean Patagonia. *In:* ELIOPOULOS, D.G. ET AL. (eds) *Mineral Exploration and Sustainable Development.* Balkema-Rotterdam, Vol I, 493–496.

GUIDO, D.M., JOVIC, S.M. & SCHALAMUK, I.B. 2005. *A new metallogenic association (Sn-Cd-In-Zn-Ag-Au) in the Deseado Auroargentiferous province, Deseado Massif, Patagonia, Argentina.* Mineral Deposit Research: Meeting the Global Challenge – 8th SGA Meeting, Beijing, China, Volume **2**, 965–968.

HEDENQUIST, J., ARRIBAS, A. & GONZÁLEZ-URIEN, E. 2000. Exploration for epithermal gold deposits. *Reviews in Economic Geology*, **13**, 245–278.

HERBST, R. 1965. La flora fósil de la Formación Roca Blanca, provincia de Santa Cruz, Patagonia, con consideraciones geológicas y estratigráficas. *Opera Lilloana*, **12**, 1–102.

JALFIN, G. & HERBST, R. 1995. La Flora triásica del Grupo El Tranquilo, provincia de Santa Cruz (Patagonia). Estratigrafía. *Ameghiniana*, **32** (3), 211–229.

JOVIC, S.M. 2009. *Geología y Metalogénesis de las mineralizaciones polimetálicas del área El Tranquilo (Cerro León), sector central del macizo del Deseado, Provincia de Santa Cruz*. Unpublished PhD thesis, Universidad Nacional de La Plata.

JOVIC, S.M., GUIDO, D.M., SCHALAMUK, I.B., MELGAREJO, J.C. & PROENZA, J. 2005. Mineralogía de veta Ivonne, deposito Cerro León: ¿Paragénesis de alta temperatura en la Provincia Auroargentifera del Deseado? XVI Congreso Geológico Argentino. *Actas*, **2**, 257–262.

OHTA, E. 1995. Common features and Genesis of Tin-polymetallic veins. *Resource Geology Special Issue*, **18**, 187–195.

PANZA, J. 1995. *Hoja geológica 4969 – II Tres Cerros escala 1: 250.000, provincia de Santa Cruz*. Dirección Nacional del Servicio Geológico, Boletín, **213**, 1–103.

PEÑALVA, G.A., JOVIC, S.M., CHERNICOFF, C.J., GUIDO, D.M. & SCHALAMUK, I.B. 2008. Cuerpos intrusivos asociados a las mineralizaciones polimetálicas del depósito Cerro León, área del anticlinal El Tranquilo, Santa Cruz: Evidencias Geofísicas. *Revista de la Asociación Geológica Argentina*, **63**(1), 14–23.

SEIFERT, T. & SANDMANN, D. 2006. Mineralogy and geochemistry of indium-bearing polymetallic vein-type deposits: Implications for host minerals from the Freiberg district, Eastern Erzgebirge, Germany. *Ore Geology Reviews*, **28**, 1–31.

SCHWARZ-SCHAMPERA, U. & HERZIG, P. 2002. *Indium. Geology, Mineralogy, and Economics*. Springer-Verlag, Berlin.

Received 30 September 2009; revised typescript accepted 14 June 2010.